http://dx.doi.org/10.15207/JKCS.2015.6.5.009

Analysis of Induced Currents on the Dielectric Cube by the Fusion of MoM and PMCHW Integral Equation

Joong-Soo Lim*
Division of Information Communication, Baekseok University

MoM과 PMCHW 적분방정식 융합에 의한 유전체 육면체의 유도전류 계산

임중수*
백석대학교 정보통신학부

Abstract In this paper, we analysis the electromagnetic scattering of an arbitrary shape dielectric cube subjected to plane wave incidence in three dimensions. MoM(Method of Moments)in which a surface of a body is divided with small triangular patches and equivalence principle are used to fuse the PMCHW(Poggio, Miller, Chang, Harrington, and Wu) Integral Equations with respect to equivalent currents on a dielectric body. Triangular patch and loop-patch basis functions that is robust in wide frequency ranges are used for MoM formulations. Proposed method is very useful to analysis the induced current of arbitrary dielectric bodies and numerical results for a dielectric cube are presented.

• Key Words : dielectric, basis function, patch, induced current, cube

요 약 본 논문에서는 유전체 표면을 소형의 패치로 분해한 다음에 각 패치의 유도전류를 구하는 모먼트법(MoM)과 전체 유전체 표면의 입사전파와 반사 및 침투 전파의 합을 구하는 적분방정식을 융합하여 유전물질로 구성된 육면체의 유도전류 분석하였다. 평면파 전자파가 입사될 때 임의모형의 유전체에 유도되는 유도전류는 일반적으로 수치해석방법을 적용하여 계산하는 것이 정확하며 사용한 적분방정식은 5 명의 과학자가 공동으로 제안한 PMCHW 방정식을 사용하였다. MoM에 사용된 패치는 삼각형 패치를 사용하고 기초함수는 광대역 주파수에 사용할 수 있는 Loop-Patch 기초함수를 사용하였다. 제안된 계산방식은 넓은 주파수 범위에서 임의 모형의 유전체에 대해서 적용할 수 있으며 유전체 육면체의 유도전류를 분석하여 제시하였다.

• Key Words :유전체, 기초함수, 패치, 유도전류, 육면체

1. Introduction

The equivalence principle is used to formulate the integral equation to solve the electromagnetic scattering from an arbitrary shape electric or dielectric body[1,2,3,4,5,6]. [Fig. 1] shows an arbitrary shape dielectric cube in a homogeneous and isotropic field. Let ε_d be the permittivity and μ_d be the permeability of the interior of the body, while ε_e and μ_e represent the parameters of the surrounding medium. Let E^i

본 논문은 백석대학교 학술연구공모과제의 지원을 받아 수행되었음.
*교신저자 : 임중수(jslim@bu.ac.kr)
접수일 2015년 8월 14일 수정일 2015년 9월 25일 게재확정일 2015년 10월 20일

represent the incident field to the scatterer and E^s represent the scattered field from the scatterer. The total field to the exterior of the body, E_e, is a summation of the incident field and the scattered field and E_d is the field in the interior[7].

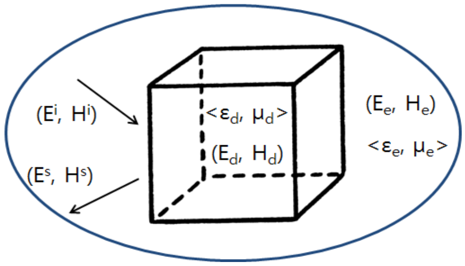

[Fig. 1] Arbitrarily shaped dielectric cube in free space.

The equivalence principle which is employed to divide the original problem into two separate problems shows in [Fig. 2] The interior problem is represented in [Fig. 2](a) and exterior problem is also represented in [Fig. 2](b). Since there is discontinuity in the fields while passing the boundary, the equivalent magnetic current(M_d) and the equivalent electrical current(J_d) are required on the surface to take care of the discontinuity.

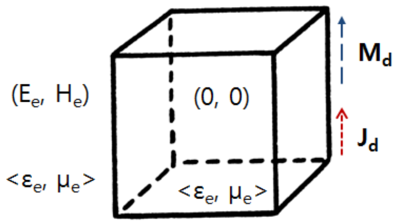

(a) Exterior equivalent problem

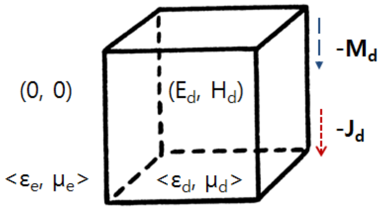

(b) Interior equivalent problem

[Fig. 2] Application of equivalent principle of dielectric body.

Since the tangential component of the electric and magnetic fields be continuous by enforcing the boundary condition, the following integral equations are derived [8,9].

$$\left[E_e^s(J_{d,}\ M_d)+E^i\right]_{\tan}=0,\ \gamma\in S^-, \tag{1}$$

$$\left[H_e^s(J_{d,}M_d)+H^i\right]_{\tan}=0,\ \gamma\in{}^-, \tag{2}$$

$$\left[E_d^s(-J_{d,}\ -M_d)\right]_{\tan}=0,\ \gamma\in S^+, \tag{3}$$

$$\left[H_d^s(-J_{d,}-M_d)\right]_{\tan}=0,\ \gamma\in S^+, \tag{4}$$

where S^- is taken to be slightly interior to S and S^+ is slightly exterior to S.

2. Fusion of PMCHW and MoM

The PMCHW formulation was made by combining Eqs. (1) with (3) and Eqs. (2) with (4), which was developed by Poggio, Miller, Chang, Harrington, and Wu[10].

$$\left[E^i\right]_{\tan}= \left[E_e^s(J_d,M_d)+E_d^s(J_{d,}M_d)\right]_{\tan},\ \gamma\in S. \tag{5}$$

$$\left[H^i\right]_{\tan}= \left[H_e^s(J_d,M_d)+H_d^s(J_{d,}M_d)\right]_{\tan}.\ \gamma\in S. \tag{6}$$

The electric and magnetic fields producted by the unknown surface current(J_d, M_d) may be written to the electric and magnetic vector and scalar potentials as following in which "−" is for $n=e$ and "+" is for $n=d$ [8].

$$E_n^s(\gamma)=\mp j\omega A_n(\gamma)\mp \nabla\Phi_n(\gamma)\mp\frac{1}{\epsilon_n}\nabla\times F_n(\gamma),\ \gamma\in S, \tag{7}$$

$$H_n^s(\gamma)=\mp j\omega F_n(\gamma)\mp \nabla\Psi_n(\gamma)\pm\frac{1}{\mu_n}\nabla\times A_n(\gamma),\ \gamma\in S, \tag{8}$$

with

$$A_n(\gamma)=\frac{\mu_n}{4\pi}\int_S J_d(\gamma')\frac{e^{-jk_nR}}{R}dS', \tag{9}$$

$$F_n(\gamma)=\frac{\epsilon_n}{4\pi}\int_S M_d(\gamma')\frac{e^{-jk_nR}}{R}dS', \qquad (10)$$

$$\Phi_n(\gamma)=\frac{1}{4\pi\epsilon_n}\int_S q^e(\gamma')\frac{e^{-jk_nR}}{R}dS', \qquad (11)$$

$$\Psi_n(\gamma)=\frac{1}{4\pi\mu_n}\int_S q^m(\gamma')\frac{e^{-jk_nR}}{R}dS'. \qquad (12)$$

We get Eq. (13) by substitute Eqs. (9) into Eqs. (5) and .get Eq. (14) by substitute Eq. (10) into Eq. (6).

$$[E^i]_{\tan}=j\omega[A_e(\gamma)+A_d(\gamma)]+[\nabla\Phi_e(\gamma)+\nabla\Phi_d(\gamma)] + \nabla\times\left[\frac{F_e(\gamma)}{\epsilon_e}+\frac{F_d(\gamma)}{\epsilon_d}\right],\ \gamma\in S, \qquad (13)$$

$$[H^i]_{\tan}=j\omega[F_e(\gamma)+F_d(\gamma)]+[\nabla\Psi_e(\gamma)+\nabla\Psi_d(\gamma)] - \nabla\times\left[\frac{A_e(\gamma)}{\mu_e}+\frac{F_d(\gamma)}{\epsilon_d}\right],\ \gamma\in S, \qquad (14)$$

In the MoM(method of moment) solution of Eqs. (13) and (14), we use the loop basis function($O_i(\gamma)$) where n_i is the edge number of the n[th] edge in loop i defined in [10,11,12], and star basis function($*_j(\gamma)$) where n_j is the edge number of the n[th] edge of a triangular patch j is defined in [13,14,15], which is also called as patch basis function [2,10].

$$O_i(\gamma)=\sum_{n_i\in loop_i}\sigma_{n_i}\frac{1}{\ell_{n_i}}\Lambda_{n_i}(\gamma) \qquad (15)$$

$$*j(\gamma)=\sum_{n_j\in face_j}\nu_{n_j}\frac{1}{\ell_{n_j}}\Lambda_{n_j}(\gamma) \qquad (16)$$

The RWG basis functions($\Lambda_n(\gamma)$) was defined in [1], where $A_n^{\pm}$ is the area of the triangular $T_n^{\pm}$.

$$\Lambda_n(\gamma)=\begin{cases}\dfrac{\ell n}{2A_n^{\pm}}\rho_n^{\pm}, & \gamma\in T_n^{\pm}\\ 0, & otherwise,\end{cases} \qquad (17)$$

If we use the same functions with testing functions, we get the testing of Eq. (13) with loop-patch basis functions as following.

$$< E^i(\gamma),O_p >=< j\omega[A_e(\gamma)+A_d(\gamma)]+ \nabla\times\left\{\frac{F_e(\gamma)}{\epsilon_e}+\frac{F_d(\gamma)}{\epsilon_d}\right],\ O_p > \qquad (18)$$

$$< E^i(\gamma),*_q >=< j\omega[A_e(\gamma)+A_d(\gamma)] + [\nabla\Phi_e(\gamma)+\nabla\Phi_d(\gamma)] + \nabla\times\left[\frac{F_e(\gamma)}{\epsilon_e}+F_d(\gamma)\frac{7}{\epsilon_d}\right],*_q >. \qquad (19)$$

Similarly, we get the testing of Eq. (14) with loop-patch basis functions as following.

$$< H^i(\gamma),O_p >=< j\omega[F_e(\gamma)+F_d(\gamma)]- \nabla\times\left[\frac{A_e(\gamma)}{\mu_e}+\frac{A_d(\gamma)}{\mu_d}\right],O_p > \qquad (20)$$

$$< H^i(\gamma),*_q >=< j\omega[F_e(\gamma)+F_d(\gamma)]- [\nabla\Psi_e(\gamma)+\nabla\Psi_d(\gamma)]- \nabla\times\left[\frac{A_e(\gamma)}{\mu_e}+\frac{A_d(\gamma)}{\mu_d}\right],*_q >. \qquad (21)$$

3. Mathematical Analysis of PMCHW Formulation

Since the current passing through the edge in the triangle patches can be represented by the sum of the currents flowing the patches and the currents flowing the loops connected to the edge, we can approximate both electric and magnetic currents as following[10].

$$J(\gamma)=\sum_i J_i^o O_i(\gamma)+\sum_j J_j^* *_j(\gamma), \qquad (22)$$

$$M(\gamma)=\sum_i M_i^o O_i(\gamma)+\sum_j M_j^* *_j(\gamma), \qquad (23)$$

where J^o_i, $J*_j$, M^o_i and M^*_j are unknown coefficients.

The next step of the numerical Analysis for J^o_i, J^*_j, M^o_i, and M^*_j is to substitute the basis functions for electric and magnetic currents and make the matrix equations[10].

$$ZI = V, \tag{24}$$

where

$$I=\begin{bmatrix} J^O \\ J^* \\ M^O \\ M^* \end{bmatrix}, \quad \text{and } V=\begin{bmatrix} V_E^O \\ V_E^* \\ V_H^O \\ V_H^* \end{bmatrix}, \tag{25}$$

$$Z=\begin{bmatrix} Z_{JJ}^{OO} & Z_{JJ}^{O*} & Z_{JM}^{OO} & Z_{JM}^{O*} \\ Z_{JJ}^{*O} & Z_{JJ}^{**} & Z_{JM}^{*O} & Z_{JM}^{**} \\ Z_{MJ}^{OO} & Z_{MJ}^{O*} & Z_{MM}^{OO} & Z_{MM}^{O*} \\ Z_{MJ}^{*O} & Z_{MJ}^{**} & Z_{MM}^{*O} & Z_{MM}^{**} \end{bmatrix}, \tag{26}$$

In Eqs. (25)-(26), $Z_{JJ}^{OO}, Z_{JJ}^{O*}, Z_{JJ}^{*O}, Z_{JJ}^{**}, Z_{JM}^{OO}, Z_{JM}^{*O}, Z_{JM}^{O*}, Z_{JM}^{**}, Z_{MJ}^{OO}, Z_{MJ}^{O*}, Z_{MJ}^{*O}, Z_{MJ}^{**}, Z_{MM}^{OO}, Z_{MM}^{O*}, Z_{MM}^{*O}$, and Z_{MM}^{**}, are submatrices, V_E^O, V_E^*, V_H^O, V_H^* are column vectors. The matrix Z may be inverted to get the unknown coefficients J^o_i J^*_j, M^o_i, and M^*_j. The matrix elements for each submatrics are given as following, where E is number of edges and F is number of faces.

$$[Z_{JJ}^{OO}]_{ji} = \frac{j\omega}{2} \sum_{m_j \in loop_j} \sum_{n_i \in loop_i} \frac{\sigma_{m_j}\sigma_{n_i}}{\ell_{n_i}} \left[A_{mn}^{ij+} \cdot \rho_{mj}^{c+} + A_{mn}^{ij-} \cdot \rho_{mj}^{c-}\right] \tag{27}$$

$$[Z_{JJ}^{*O}]_{ji} = \frac{j\omega}{2} \sum_{m_j \in face_j} \sum_{n_i \in loop_i} \frac{\nu_{m_j}\sigma_{n_i}}{\ell_{n_i}} \left[A_{mn}^{ij+} \cdot \rho_{mj}^{c+} + A_{mn}^{ij-} \cdot \rho_{mj}^{c-}\right]. \tag{28}$$

$$[Z_{JJ}^{O*}]_{ji} = \frac{j\omega}{2} \sum_{m_j \in loop_j} \sum_{n_i \in face_i} \frac{\sigma_{m_j}\nu_{n_i}}{\ell_{n_i}} \left[A_{mn}^{ij+} \cdot \rho_{mj}^{c+} + A_{mn}^{ij-} \cdot \rho_{mj}^{c-}\right]. \tag{29}$$

$$[Z_{JJ}^{**}]_{ji} = \frac{j\omega}{2} \sum_{m_j \in face_j} \sum_{n_i \in face_i} \frac{\nu_{m_j}\nu_{n_i}}{\ell_{n_i}} \left[A_{mn}^{ij+} \cdot \rho_{mj}^{c+} + A_{mn}^{ij-} \cdot \rho_{mj}^{c-}\right] + \left[\Phi_{mn}^{ij-} - \Phi_{mn}^{ij+}\right], \tag{30}$$

$$[Z_{JM}^{OO}]_{ji} = \frac{j\omega}{2} \sum_{m_j \in loop_j} \sum_{n_i \in loop_i} \frac{\sigma_{m_j}\sigma_{n_i}}{\ell_{n_i}} \nabla \times \left[\frac{F_{mn}^{ij+}}{\epsilon} \cdot \rho_{mj}^{c+} + \frac{F_{mn}^{ij-}}{\epsilon} \cdot \rho_{mj}^{c-}\right], \tag{31}$$

$$[Z_{JM}^{*O}]_{ji} = \frac{j\omega}{2} \sum_{m_j \in face_j} \sum_{n_i \in loop_i} \frac{\nu_{m_j}\sigma_{n_i}}{\ell_{n_i}} \nabla \times \left[\frac{F_{mn}^{ij+}}{\epsilon} \cdot \rho_{mj}^{c+} + \frac{F_{mn}^{ij-}}{\epsilon} \cdot \rho_{mj}^{c-}\right], \tag{32}$$

$$[Z_{JM}^{O*}]_{ji} = \frac{j\omega}{2} \sum_{m_j \in loop_j} \sum_{n_i \in face_i} \frac{\sigma_{m_j}\nu_{n_i}}{\ell_{n_i}} \nabla \times \left[\frac{F_{mn}^{ij+}}{\epsilon} \cdot \rho_{mj}^{c+} + \frac{F_{mn}^{ij-}}{\epsilon} \cdot \rho_{mj}^{c-}\right], \tag{33}$$

$$[Z_{JM}^{**}]_{ji} = \frac{j\omega}{2} \sum_{m_j \in face_j} \sum_{n_i \in face_i} \frac{\nu_{m_j}\nu_{n_i}}{\ell_{n_i}} \nabla \times \left[\frac{F_{mn}^{ij+}}{\epsilon} \cdot \rho_{mj}^{c+} + \frac{F_{mn}^{ij-}}{\epsilon} \cdot \rho_{mj}^{c-}\right], \tag{34}$$

$$[Z_{MJ}^{OO}]_{ji} = \frac{j\omega}{2} \sum_{m_j \in loop_j} \sum_{n_i \in loop_i} \frac{\sigma_{m_j}\sigma_{n_i}}{\ell_{n_i}} \nabla \times \left[\frac{A_{mn}^{ij+}}{\mu} \cdot \rho_{mj}^{c+} + \frac{A_{mn}^{ij-}}{\mu} \cdot \rho_{mj}^{c-}\right], \tag{35}$$

$$[Z_{MJ}^{*O}]_{ji} = \frac{j\omega}{2} \sum_{m_j \in face_j} \sum_{n_i \in loop_i} \frac{\nu_{m_j}\sigma_{n_i}}{\ell_{n_i}} \nabla \times \left[\frac{A_{mn}^{ij+}}{\mu} \cdot \rho_{mj}^{c+} + \frac{A_{mn}^{ij-}}{\mu} \cdot \rho_{mj}^{c-}\right], \tag{36}$$

$$[Z_{MJ}^{O*}]_{ji} = \frac{j\omega}{2} \sum_{m_j \in loop_j} \sum_{n_i \in face_i} \frac{\sigma_{m_j}\nu_{n_i}}{\ell_{n_i}} \nabla \times \left[\frac{A_{mn}^{ij+}}{\mu} \cdot \rho_{mj}^{c+} + \frac{A_{mn}^{ij-}}{\mu} \cdot \rho_{mj}^{c-}\right], \tag{37}$$

$$[Z_{MJ}^{**}]_{ji} = \frac{j\omega}{2} \sum_{m_j \in face_j} \sum_{n_i \in face_i} \frac{\nu_{m_j}\nu_{n_i}}{\ell_{n_i}} \nabla \times \left[\frac{A_{mn}^{ij+}}{\mu} \cdot \rho_{mj}^{c+} + \frac{A_{mn}^{ij-}}{\mu} \cdot \rho_{mj}^{c-}\right], \tag{38}$$

$$[Z_{MM}^{OO}]_{ji} = \frac{j\omega}{2} \sum_{m_j \in loop_j} \sum_{n_i \in loop_i} \frac{\sigma_{m_j}\sigma_{n_i}}{\ell_{n_i}} \left[F_{mn}^{ij+} \cdot \rho_{mj}^{c+} + F_{mn}^{ij-} \cdot \rho_{mj}^{c-}\right], \tag{39}$$

$$[Z_{MM}^{*O}]_{ji} = \frac{j\omega}{2} \sum_{m_j \in face_j} \sum_{n_i \in loop_i} \frac{\nu_{m_j}\sigma_{n_i}}{\ell_{n_i}} \left[F_{mn}^{ij+} \cdot \rho_{mj}^{c+} + F_{mn}^{ij-} \cdot \rho_{mj}^{c-}\right] \tag{40}$$

$$[Z_{MM}^{O*}]_{ji} = \frac{j\omega}{2} \sum_{m_j \in loop_j} \sum_{n_i \in face_i} \frac{\sigma_{m_j}\nu_{n_i}}{\ell_{n_i}} \left[F_{mn}^{ij+} \cdot \rho_{mj}^{c+} + F_{mn}^{ij-} \cdot \rho_{mj}^{c-}\right], \tag{41}$$

$$[Z_{MM}^{**}]_{ji} = \frac{j\omega}{2} \sum_{m_j \in face_j} \sum_{n_i \in face_i} \frac{\nu_{m_j}\nu_{n_i}}{\ell_{n_i}} \left[F_{mn}^{ij+} \cdot \rho_{mj}^{c+} + F_{mn}^{ij-} \cdot \rho_{mj}^{c-}\right] + \left[\Psi_{mn}^{ij-} - \Psi_{mn}^{ij+}\right] \tag{42}$$

Similarly, the elements of V_E^O, V_H^o, V_E^*, and V_H^* are given by

$$[V_E^O]_j = \sum_{m_j \in loop_j} \left[E_{m_j}^+ \cdot \rho_{m_j}^{c+} + E_{m_j}^- \cdot \rho_{m_j}^{c-} \right], \tag{43}$$

$$[V_E^*]_j = \sum_{m_j \in patch_j} \left[E_{m_j}^+ \cdot \rho_{m_j}^{c+} + E_{m_j}^- \cdot \rho_{m_j}^{c-} \right], \tag{44}$$

$$[V_H^O]_j = \sum_{m_j \in loop_j} \left[E_{m_j}^+ \cdot \rho_{m_j}^{c+} + E_{m_j}^- \cdot \rho_{m_j}^{c-} \right], \tag{45}$$

$$[V_H^*]_j = \sum_{m_j \in patch_j} \left[E_{m_j}^+ \cdot \rho_{m_j}^{c+} + E_{m_j}^- \cdot \rho_{m_j}^{c-} \right]. \tag{46}$$

The currents calculating in Eqs. (22) and (23) may be evaluated by the numerical procedures described in [10].

4. Numerical Results and Conclusion

We analysis the induced currents of the dielectric cube which is illuminated by a 60MHz x-polarized plane wave in [Fig. 3]. The cube is 1.0m on a side and has a dielectric constant ε_γ=2.0). The cube is divided into 5, 5 and 4 divisions along x, y and z-directins, and these divisions result in 296 triangles resulting in 888 unknowns in the MOM solution[10].

[Fig. 4] compares the equivalent currents J on the top surface of the cube along two principal cuts obtained from the edge and loop-patch methods. The dielectric cube is illuminated by a z-traveling x-polarized plane wave (f=60MHz). The comparison is excellent.

[Fig. 5] shows the comparison of equivalent currents M for the previous case and again the comparison is excellent.

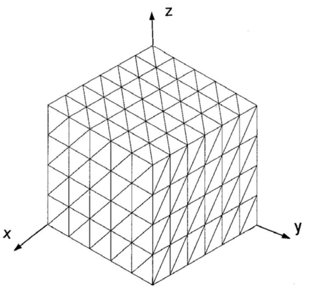

[Fig. 3] A triangulated model of the dielectric cube (ε_γ=2.0, a=1.0m), unknowns =888.

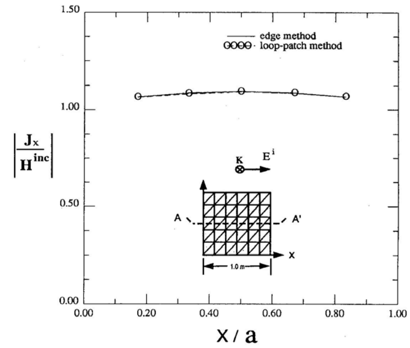

[Fig. 4] The x-component of the equivalent electric current induced on the dielectric cube illuminated by x-polarized plane wave traveling along the z-axis. ε_γ=2.0, λ =5.0m, Number of unknowns=888.

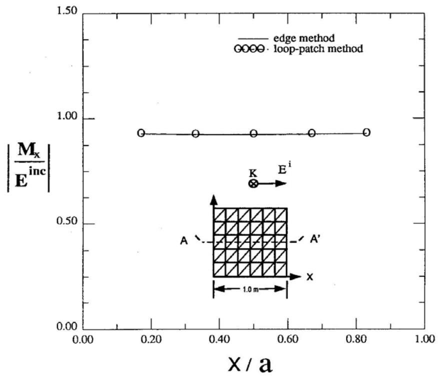

[Fig. 5] The x-component of the equivalent magnetic current on the dielectric cube.

ACKNOWLEDGMENTS

본 논문은 2015년도 백석대학교 학술연구공모과제의 지원을 받아 수행된 것임

REFERENCES

[1] S. M. Rao, D. R. Wilton, A. W. Glisson, "Electromagnetic Scattering by Surfaces of Arbitrary Shape", IEEE Transactions on Antenna and Propagation, Vol. AP-30, pp. 409-418, 1982.

[2] Joong-Soo Lim, Gyoo-Soo Chae, "Electromagnetic

Scattering from Dielectric Bodies at Very Low Frequency Range Using Loop-Star Basis Functions', International Journal of Applied Engineering Research, Vol. 9, No. 22, pp. 8233-8243, 2014.

[3] S. M. Rao, C, C. Cha, R. L. Cravey, "Electromagnetic Scattering from Arbitrary Shaped Conducting Bodies Coate3d with Lossy materials of Arbitrary Thickness", IEEE Transactions on Antenna and Propagation, Vol. AP-39, pp. 627-631, 1991.

[4] K. S. Yee, "Numerical Solution of Initial Boundary Value Problems Involving Maxwell's Equations in Isotrophic Media", IEEE Transactions on Antenna and Propagation, Vol. AP-14, pp. 302-307, 1966.

[5] T. Cwik, "Coupling Finite Element and Integral Solutions Using Decoupled Boundary Meshed", IEEE Transactions on Antenna and Propagation, Vol. AP-40, pp. 1496-1504, 1992.

[6] D. A. Vechinski, S. M. Rao, "A Stable Procedure to Calculate the Transient Scattering by Conducting Surfaces of Arbitrary Shape", IEEE Transactions on Antenna and Propagation, Vol. AP-40, pp. 661-665, 1992.

[7] E. H. Newman and D. M. Pozer, "Electromagnetic Modeling of Composite Wire and Surface Geometries", IEEE Transactions on Antenna and Propagation, Vol. AP-26, pp. 784-789, 1978.

[8] R. F. Harrington, Time-Harmonic Electromagnetic Fields, McGraw-Hill, New York, 1982.

[9] R. F. Harrington, Field Computation by Moment Methods, New York, Macmillian 1968.

[10] Joongsoo Lim, "The Electromagnetic Scattering from Arbitrarily Shaped Bodies at Very Low Frequency Range Using Triangular Patch Modeling", PhD Dissertation, Auburn University, 1994.

[11] Savas Uckun, Tapan K. Sarkar, Sadasiva M. Rao, "A Novel Technique for Analysis of Electromagnetic Scattering from Microstrip Antennas of Arbitrary Shape", IEEE Transactions on Microwave Theory and Techniques, Vol. 45, No. 4, pp. 485-491, 1997.

[12] Jin-Fa Lee, Robert Lee, Robert J. Burkholder, "Loop Star Basis Functions and a Robust Preconditioner for EFIE Scattering Problems", IEEE Transactions on Antenna and Propagation, Vol. 51, No. 8, pp. 1853-1863, 2003.

[13] N. Kurt-Karsilayan, K. A. Michalski, "A Full-wave Wide-band Surface-integral-equation-based Field solver", PIERS Online, Vol. 4, No. 8, 2008.

[14] Ji-Hwan Hwang, Soon-Koo Kweon, Yisok Oh, "Angular Effect of Virtual Vertices Inserted to Treat on an Infinite Conducting Surface", Journal of Electromagnetic Engineering and Science, KIEES, Vol. 13, No. 1, pp. 16-21, 2013.

[15] Nefi A. Barron Herrera, Javier A. Castaneda Nunez, E. R. Sanchez, "Electromagnetic Field Interaction with a Dielectric Body of Ellipsoidal Shape", CCE2008, pp. 234-237, 2008.

저자소개

임 중 수(Joong-Soo Lim) **[종신회원]**

• 1994년 3월 : Auburn대학교 전자공학과 (공학박사)
• 1994년 3월 ~ 2003년 2월 : 국방과학연구소 책임연구원, 전자전연구실 실장
• 2003년 3월 ~ 현재 : 백석대학교 정보통신학부 교수
• 2007년 3월 ~ 현재 : 한국전자파학회 평의원

<관심분야> : IT융합, 정보통신, 전자기기, 전자전, 수치해석